Effect of Flap Mutation I54L/M in Inhibition of Human Immunodeficiency Virus Type 1 Protease: Relationship to Drug Resistance

Rituraj Purohit and Rao Sethumadhavan*

Bio-informatics Division ,School of Bio Sciences and Technology (SBST), Vellore Institute of Technology University, Vellore, Tamil Nadu, India

Abstract

The HIV-1 protease enzyme is one of the prime and an utmost essentially important target towards the HIV therapy. However, one of the most complex mechanisms found in this enzyme is that, it produces resistance toward most of the drugs due to mutational changes, but still maintains activity with their natural substrates. This work focuses on mechanism of Darunavir resistance HIV-1 protease flap mutant I54M and I54L. To gain insight into why mutations confer such resistance, Docking analysis, binding energetics analysis and Molecular Dynamics simulations in explicit solvent were performed on drug resistant mutants and native HIV-1 protease. The flap mutation I54M and I54L lowers the binding affinity of Darunavir by altering the position of binding site residues in 3D space. It decreases the electrostatic and van der waals interaction energy and further reduction in total receptor-ligand interaction energy. In Darunavir resistance, the contribution of I54M mutant was more than I54L mutant. The results summarized in this paper emphasize the importance of shape complementarity and flexibility of binding residues in drug design.

Introduction

Human immunodeficiency virus type 1 (HIV-1) encodes a 22 kDa homodimeric aspartic protease that cleaves the *gag* and *pol* viral polyproteins at nine specific sites and thus permits viral maturation (Kohl et al., 1988). HIV-1 protease is one of the most extensively studied enzymes, both experimentally and computationally. Hence, the invention of drugs that restrict proteolytic processing by the protease is a prime goal in the treatment of HIV-1 infection. Nine commercially available drugs are based on the inhibition of this enzyme to treat acquired immune deficiency syndrome (AIDS) (Wensing et al., 2010). The clinical success of these drugs is hindered by the frequent occurrence of drug-resistant mutations of the HIV-1 protease. The resistant strains encode mutated proteases with reduced binding affinity for the inhibitors but with sufficient enzymatic activity to process the viral polyproteins. However, the emergence of active, drug-resistant mutants of the protease has limited the long-term effectiveness of these inhibitors. Thus, the design of HIV-1 protease inhibitors with novel mechanisms of action and reduced resistance liabilities is still desirable.

An important structure feature of the aspartic proteinases is the short antiparallel β-sheet with a turn known as flap. The homodimer HIV-1 protease molecule possesses two flaps. The flaps of the protease (residues 33–62) must open for segments of the polyprotein to access the active site. Once the appropriate region of the polyprotein is in the active site, the flaps must close over the substrate sequence for cleavage to occur. The catalytic residues of HIV-1 protease are located at the bottom of a large open cavity, the ceiling of which is composed of 2 flaps, one from each monomer. Although the structure and function of HIV-1 PR have been studied for over 20 years, questions remain regarding the conformations and dynamics of the flaps that cover the active site cavity. The flaps of the protease must open for segments of the polyprotein to access the active site. Once the appropriate region of the polyprotein is in the active site, the flaps must close over the substrate sequence for cleavage to occur, it is shown in Figure 1. Fascinatingly, the flaps are reversed into a closed conformation in the ligand bound protease compared to the ligand free enzyme, which suggests that an extensive conformational change takes place upon ligand binding (Wlodawer et al., 1989; Miller et al., 1989; Rick et al., 1998). Understanding the issues that govern HIV-1 protease flap mutation and effect to the binding residues has profound implications for elucidating the detailed mechanism of this enzyme and in the design of new therapeutic agents, such as allosteric inhibitors intended to interfere with flap opening and thereby with enzymatic function. Thus, numerous prior computational studies have aimed at understanding flap opening dynamics. Reported results from activated molecular dynamics (MD) simulations in the gas phase that involved forcing the atomic coordinates for non flap regions of a closed structure to the semi open state (Collins et al., 1995). Darunavir, formerly TMC-114, is the latest approved protease inhibitor (PI) for the treatment of HIV infection. It was originally designed to be active against HIV strains resistant to other currently available PIs. In the latest International AIDS Society-USA panel list (www.iasusa.org, last update in December 2008), a total of 11 mutations were defined as specifically associated with Darunavir resistance. They were segregated as major (I50V, I54M, L76V and I84V) or minor (V11I, V32I, L33F, I47V, I54L, G73S and L89V) resistance mutations (Johnson et al., 2008). The enzyme shows the resistance, if the mutation is able to change the 3D space of binding cleft.

The mechanism behind Darunavir resistance inhibition is not well

***Corresponding author:** Rao Sethumadhavan, Bio-informatics Division ,School of Bio Sciences and Technology (SBST), Vellore Institute of Technology University, Vellore, Tamil Nadu, India, Tel: +91-416-2202522, 2202523; Fax: +91-416-2243092; E-mail: rsethumadhavan@vit.ac.in

understood, but the variants do have mutations in both the active site and nonactive site regions. The inhibition can be accomplished by disturbing favorable ligand protein interactions in the binding pocket. However, accumulating evidence suggests that the flap region also plays an important role in influencing both substrate and inhibitor binding/stability (Scott and Schiffer, 2000; Clemente et al., 2004). Another possibility for resistance is that the active site specificity itself is reduced because of a mutation(s) in the flap region preventing flap closure, inducing an expansion of the active site cavity.

We carry out computer simulations in the hope of understanding the properties of assemblies of molecules in terms of their structure and the microscopic interactions between them. Molecular dynamics simulations can be used to predict the effects of mutations on the protease structure. Molecular dynamics simulations of HIV protease have been used to evaluate the catalytic mechanism and the structural flexibility (Harrison and Weber, 1994; Liu et al., 1996; Trylska, 2004). Here, molecular dynamics simulations of solvated native and two mutants protease were run in order to better model the solution behavior and to evaluate the physical basis for drug resistance.

In this study we carry out docking and binding energetics analysis of HIV-1 native and flap mutant structures with respect to Darunavir. To understand the above mention analysis result we performed explicit solvent molecular dynamics (MD) simulations starting from a native HIV-1 protease crystal structure and two resistance flap mutant (I54L and I54M). Overall, the native and mutants proteases ultimately deviate from their respective crystal structures to a similar extent. However, the native exhibits a more localized structural change than the mutants that begins around 2 ns after initiation of the simulation. The mutants alter its overall configuration from the crystal structure very quickly relative to the native. The fast configuration change in structure of mutants, alters 3D conformation of binding residues might be the cause of resistance toward Darunavir.

Materials and Methods

Data set

We selected native HIV-1 protease (PDB ID 1ODW) (Kervinen et al., 1996) structu res from Brookhaven Protein Data Bank (Berman et al., 2000), and one small molecule/inhibitor, Darunavir for our investigation. We induced two point mutation at 54th position isoleucine to leucine and methionin in native structure to build mutant structures and the energy was minimized by normad server (Lindahl et al., 2006) with default parameters. The native structure also subject to the same in silico mutation methods, where the native residue is mutated to itself, to ensure that this mutation procedure is not introducing an artifact. We called I54I as mutant 1 and I54M as mutant 2 in our paper. Isoleucin locating at 54th position at flap region and above mutant at this position produce the resistance against Darunavir (King et al., 2004; Ghosh et al., 2007). The SMILES string of Darunavir were collected from PubChem, a database maintained in NCBI (Feldman et al., 2006), and submitted to CORINA (www.molecularnetworks.com/online demos/corina demo.html) for constructing the 3D structure of small molecule.

Determination of binding pocket and sequence comparison

An accurate description of protein shape derived from protein structure is necessary to establish an understanding of protein-ligand interactions, which in turn will lead to improved methods for protein-ligand docking and binding site analysis. Shape descriptors representing protein structure, such as depth (Coleman et al., 2005;

Nayal and Honig, 2006), surface curvature (Coleman and Sharp, 2006), extreme elevation (Agarwal et al., 2004), surface area and volume (Liang et al., 1998), have been used extensively to identify, study and compare protein ligand interactions, protein-protein interactions and the respective binding sites. We have used CASTp server (Dundas et al., 2006), to determine the binding pocket. CASTp server uses the weighted Delaunay triangulation and the alpha complex for shape measurements. It provides identification and measurements of surface accessible pockets as well as interior inaccessible cavities, for proteins and other molecules. It measures analytically the area (in Å²) and volume (in Å³) of each pocket and cavity, both in solvent accessible surface (SA, Richards' surface) and molecular surface (MS, Connolly's surface). We set probe radius of 1.4 Å as default value. The detected pockets from these algorithms ranked with their volumes and areas. For ligand molecules internal protein cavities appear to be a favored binding sites (Eckenhoff and Johansson, 1997), and the cavity volume may play an important role in the strength of the guest molecule–host cavity interaction. In CASTp analysis, we have chosen the first pocket for our analysis, based on volume of the pocket. Sequence comparison is one of the parameter to understand the residual arrangement of protein. We performed multiple sequence alignment by ClustalW (Thompson et al., 1994) to check the position of active site residues in native and flap mutants.

Computation of docking score and interaction energy between the inhibitor and HIV-1 protease enzyme

We used the web server PatchDock (Duhovny et al., 2005) to compute the scores of docked complexes. 3D coordinates of all the individual HIV-1 protease and the inhibitor was submitted in PDB format with default parameters. In docking Asp29, Asp30, Asp128 and Asp129 residues acting as binding residues and participate in ligand interaction (Ghosh et al., 2007; Feldman et al., 2006) . The neighboring residues were given to address the active site inside receptor and better access of ligand molecule. The underlying principle of this server is based on molecular shape representation, surface patch matching plus filtering and scoring (Duhovny et al., 2002). It is aimed at finding docking transformations that yield good molecular shape complementarity. Such transformations, when applied, induce both wide interface areas and small amounts of steric clashes. A wide interface is ensured to include several matched local features of the docked molecules that have complementary characteristics. The Patch-Dock algorithm divides the Connolly dot surface representation (Connolly 1983a; Connolly 1983b) of the molecules into concave, convex and flat patches. Then complementary patches are matched in order to generate candidate transformations. Each candidate transformation is further evaluated by a scoring function that considers both geometric fit and atomic desolvation energy (Zhang et al., 1997). Finally, an RMSD (root mean square deviation) clustering is applied to the candidate solutions to discard redundant solutions. The main reason behind PatchDock's high efficiency is its fast transformational search, which is driven by local feature matching rather than brute force searching of the six-dimensional transformation space. It further speeds up the computational processing time by utilizing advanced data structures and spatial pattern detection techniques, such as geometric hashing and pose clustering. The interaction energy of the complex was calculated by PEARL web server (Han et al., 2006). The server compute total ligand-receptor interaction energy and its components are computed by an atomic level molecular mechanics-based force field involving intermolecular van der Waals, electrostatic and hydrogen bond interactions between the binding molecule and its receptor. The electrostatic energy is particularly well suited for

analyzing recognition process because it is a physically meaningful representation of how a molecule is perceived by another molecule in its vicinity. It is through their mutual electrostatic interactions that the two molecules involved in the interaction first 'see' each other. The electrostatic energy is the only long-range non-bonded interaction and its value is calculated for pairs of atoms that are separated by three or more bonds. Thus it is assumed that the well-separated atoms are interacting mainly electro-statically since no cut-off distance was used in the calculation of the electrostatic interactions (Politzer and Muray, 1991; Naray-Szabo and Ferenczy, 1995). The negative value of electrostatic energy enables better interaction and vice-versa. The proper formation of hydrogen bonds and van der Waals contacts require complementarity of the surfaces involved. Such surfaces must be able to pack closely together, creating many contact points, and charged atoms must be properly positioned to make electrostatic bonds. Thus van der Waals and polar interactions contribute to the dynamic stability of the ligand-receptor complex (Chothia and Janin, 1975; Getzoff et al., 1992; Jacob, 1992)

Individual receptor and the ligand molecule were given as input for performing the docking experiments. The default RMSD value (4.00 Å) was used and we given the receptor binding site residues information docking experiments. The complex structure file was given as input to PEARLS web server to perform the interaction analysis.

Solvent accessibility analysis

Solvent accessibility is the ratio between the solvent accessible surface area of a residue in three-dimensional structures and that in an extended tripeptide conformation (Fraczkiewicz and Braun, 1998). It indicates the packing arrangement of residues. The solvent accessible surface area is defined as the locus of the centre of the solvent molecule as it rolls over the van der Waals surface of the protein. It is typically calculated using the 'rolling ball' algorithm (Shrake and Rupley, 1973). The accessible molecular surface is determined for a probe with a radius of 1.4 Å. It is the major intermediate step to understand the structure–function relationships of proteins. The location of amino acid residues in protein structures paves a way to determine their influence on interaction with other residues/surrounding medium and hence the folding and stability of proteins.

We obtained the solvent accessibility information by using ASAView (Ahmad et al., 2004). Solvent accessibility was divided predominantly into buried and exposed region indicating, the least accessibility and high accessibility of the amino acid residues to the solvent, respectively (Gilis and Rooman, 1996; Gilis and Rooman, 1997). The term buried surface area has two related meanings first the surface buried away from solvent when the protein folds, and second the surface buried away from solvent when two proteins or subunits associate to form a complex. We have analyzed native and mutants and observed the solvent accessibility of binding residues, before and after docking analysis.

Molecular dynamics simulation

Molecular dynamics simulations were performed using the GROMACS 4.0.5 (Hess et al., 2008; Spoel et al., 2005) running on a single 2.8 GHz Pentium IV IBM machine with 512 MB RAM and running Fedora Core 2 Linux package and GROMOS96 (Gunsteren et al., 1996) 43a1 force field implemented on LINUX architecture. 3D Structure coordinates of native HIV-1 protease and two mutants I54L and I54M were used as starting point for MD simulations.

Crystallographic waters were not included. The protein was solvated in a cubic 0.9 nm of 15960 SPC (Berendsen et al., 1981) water molecules. At physiological pH, the protein is positively charged, thus in order to make the simulation system electrically neutral, we added four chloride ions (Cl-) to the simulation box using the "genion" tool that accompanies Gromacs. The simulation system was set up as an NPT ensemble, i.e., constant number of particles (N), constant pressure (P) and constant temperature (T). All protein atoms were at a distance equal to 1.0 nm from the box edges. The system was subjected to energy minimization for 1000 steps by steepest descent. The minimized system was equilibrated for 100 ps each at 300 K by position restrained molecular dynamics simulation in order to permit waters to diffuse into the cavity to prevent the collapse (Meagher and Carlson, 2005). The equilibrated systems were then subjected to molecular dynamics simulations for 1500 ps each at 300 K. In all simulations, the temperature was kept constant at 300 K with a Berendsen thermostat (Berendsen et al., 1984). The particle mesh Ewald method (Essmann et al., 1995) was used to treat long-range Coulombic interactions and the simulations performed using the SANDER module (Case et al., 2002). The ionization states of the residues were set appropriate to pH 7 with all histidines assumed neutral. The SHAKE algorithm was used to constrain bond lengths involving hydrogens, permitting a time step of 2 fs. Van der Waals and coulomb interactions were truncated at 1.0 nm. The non-bonded pair list was updated every 10 steps and conformations were stored every 0.5 ps. Other analyses were performed using scripts included with the Gromacs (Hess et al., 2008) distribution. The visual analysis of protein structures was carried out using (Rasmol Sayle and Millner-White, 1995).

The major focus of this study is to compare the dynamic behaviors of native and mutant protein at 300 K. To that end we compare root mean square fluctuation (RMSF) of carbon alpha and root mean square deviation (RMSD) of backbone structure of protein between the trajectories generated at 300 K to explore the flexible nature of mutant.

In order to generate the three-dimensional backbone root mean square deviation (RMSD) and RMSF of carbon alpha carbon of the system were plotted for all three simulations using GRACE program (version 5.1.22).

Result

We report the pocket volume of native and mutant HIV-1 protease
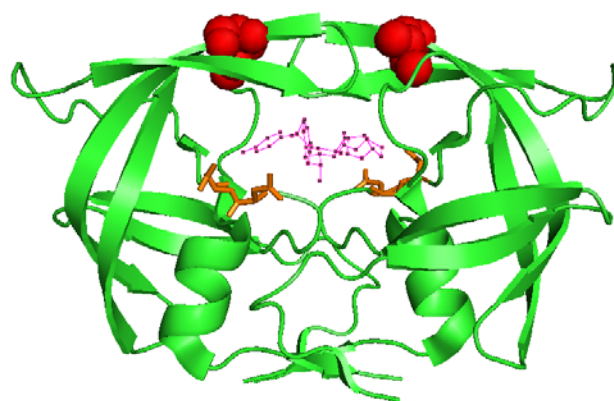
Figure 1: HIV-1 protease native complex (in cartoon) with binding residues Asp29 and Asp30 (in sticks), ligand molecule (in lines) and the site of mutation at flap region residue Ile54 (in spheres) generated by pyMOL (www.pymol.org).

```
Native      PQVTLWQRPLVTIKIGGQLKEALLDTGADDTVLEEMSLPGRWKPKMIGGIGGFIKVRQYD  60
Mutant1     PQVTLWQRPLVTIKIGGQLKEALLDTGADDTVLEEMSLPGRWKPKMIGGIGGFLKVRQYD  60
Mutant2     PQVTLWQRPLVTIKIGGQLKEALLDTGADDTVLEEMSLPGRWKPKMIGGIGGFMKVRQYD  60
            ********************************************************:******

Native      QILIEICGHKAIGTVLVGPTPVNIIGRNLLTQIGCTLNF  99
Mutant1     QILIEICGHKAIGTVLVGPTPVNIIGRNLLTQIGCTLNF  99
Mutant2     QILIEICGHKAIGTVLVGPTPVNIIGRNLLTQIGCTLNF  99
            **************************************
```

Figure 2: Sequence comparison of native and mutants, ':' and '*' indicate the conserved substitution and identical residue, respectively.

Protein structure	Total Cavity Volume (in Å³)	Docking Score	Ligand-Receptor Electrostatic Energy (in Kcal/mol)	Ligand-Receptor Van der Waals Energy (in Kcal/mol)	Total Ligand-Receptor Interaction Energy (in Kcal/mol)	Solvent accessibility at binding residues	
						Before docking	After docking
Native	299.8	7208	-0.18	-5.13	-7.28	Buried	Exposed
Mutant 1	940.7	6800	-1.28	-3.17	-6.34	Buried	Exposed
Mutant 2	959.3	6532	-1.97	-0.40	-4.80	Buried	Exposed

Table 1: Total cavity volume, Docking score, ligand–receptor interaction energy and solvent accessibility analysis at binding residues of wild and flap mutants.

enzymes. Appropriate cavity volume gives better accommodation of ligand molecule inside the pocket. We found considerable difference in pocket volume of native, mutant 1 and mutant 2 as 299.8, 940.7 and 959.3 (in Å³) respectively. We evaluated solvent accessibility and performed the molecular dynamics simulation of native and mutants structure to explore the conformation changes with respect to time. We highlighted the RMSF of Asp29, Asp30, Asp128 and Asp129 act as binding residue for Darunavir in HIV-1 protease enzyme (King et al., 2004; Ghosh et al., 2007). Our present study also endorses this experimentally observed fact. During sequence comparison analysis binding residues position was found identical in native and mutants, it is shown in Figure 2. Our investigation showed the behavior of protein–ligand complex of HIV-1 protease enzyme with Darunavir. Docked native HIV-1 protease complex is shown in Figure 1. The docking score of complex of Darunavir with native, mutant 1 and mutant 2 are found to be 7208, 6800 and 6532 respectively (Table 1).

Van der waals and electrostatic energy contributed major part with -0.18 and -5.13 kcal/mol in total ligand receptor interaction energy of native HIV-protease complex that is -7.28 kcal/mol. Van der waals and electrostatic energy confirms significant amount of complementarities between native receptor and Darunavir. While in mutant 1 has less van der waals and less electrostatics energy as -1.28 and -3.17 kcal/mol to total interaction energy -6.34 kcal/mol. Further reduction in both energies in mutant 2 given total interaction energy of -4.80 kcal/mol (Table 1). It proves that deviation from actual position of binding residues (Asp29, Asp30, Asp128' and Asp129') may be the reason of reduction in interaction energy and gradual decrease in docking score.

We found that binding residues in all the mutants is located in buried regions before docking and exposed region after docking (Table 1). During the process of docking the buried binding residues are being exposed and the cavity is occupied with inhibitor molecule.

We have performed molecular dynamics simulation of each native and mutant to observe the deviation of each atom of mutant as well as native structure in water with respect to time to explore the flexible nature of binding residues. In this analysis we evaluated RMSD of backbone and RMSF of C-alpha carbon.

In the trajectory of native RMSD change significantly up to 200 ps after which it remains the same till 13 ns and increases slightly and attains a value ~0.15 nm at 1500 ps. In the trajectory of mutant 1 structure backbone RMSD increases slightly from the starting conformation, which fluctuates, between 0.1 nm and ~0.18 nm during the simulation. Mutant 2 RMSD does not change significantly up to 200 ps after which it change from 0.13 nm to 0.17 nm at 220 ps and attain a value 0.22 nm at 1500 ps. These results are summarized in Figure 3.

RMS fluctuations have been calculated for 1500 ps. We computed the RMS fluctuations per residue over the production run of native and mutant structures, It is shown in Figure 4. We found that the

Protein structure	Root mean-square fluctuation of alpha-carbon at binding residues (in nm)			
	Asp29	Asp30	Asp128'	Asp129'
Native	0.082	0.079	0.059	0.056
Mutant 1	0.073	0.069	0.066	0.067
Mutant 2	0.100	0.068	0.132	0.119

Table 2: Root mean-square fluctuation of alpha-carbon atom (in nm) of binding residues in chain A and Chain B of native and mutants.
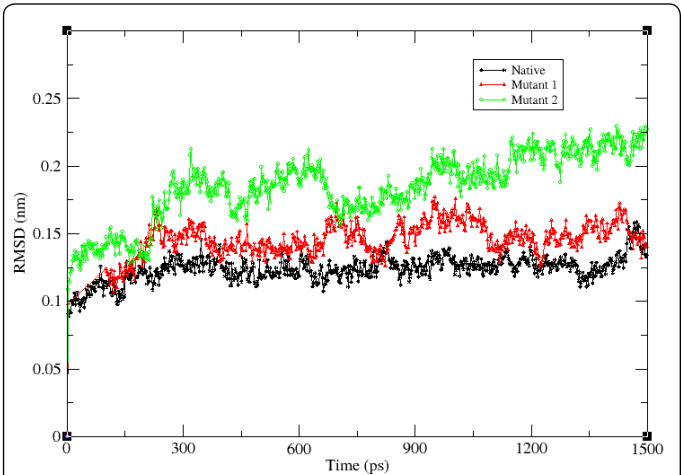
Figure 3: Time evolution of Backbone RMSDs are shown as a function of time of the native and mutant structures at 300 K. The symbol coding scheme is as follows: native (as star), mutant 1 (as triangle) and mutant 2 (as circle).

Figure 4: Time evolution of Backbone RMSFs of carbon alpha coordinates are shown as a function of residue number of the native and mutant structures at 300 K. The symbol coding scheme is as follows: native (as star), mutant 1 (as triangle) and mutant 2 (as circle).
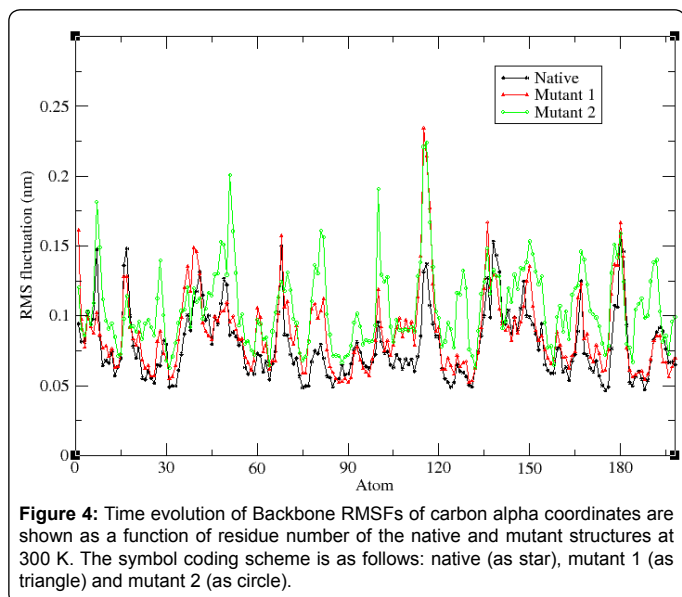
average RMS atomic fluctuation in native does not exceed 0.15 nm, while in mutant 1 and mutant 2 it cross by 0.20nm and 0.23 nm.

In native structure the RMS fluctuation at binding residues in chain A and chain B was observed minimum and maximum in mutant 2 structure. Mutant 1 made intermediate RMS fluctuation (Table 2).

Discussion

Pocket analysis shown the expansion of cavity form native to mutant structures. This expanded cavity reduces the fit of inhibitors and lowers the binding affinity by decreasing van der Waals contacts and hydrogen bonding. Higher the docking score shows better complementarity between receptor and drug molecule. Docking score of native type structure was highest as compare to mutant type, it indicates good agreement between receptor and Darunavir. Lowest docking score of mutant 2 indicate least complementarity. We computed the total interaction energy of the complex significantly contributed by van der waals and electrostatic interaction energy between HIV-1 protease (native and mutant) and Darunavir. Lower energy of the complex shows the better interaction and good agreement between receptor and ligand molecule. Estimates of VDW interaction energy were computed to provide a theoretical quantitative assessment for the ligand-protease non-bonded interactions. The two factors, namely, score difference in docking process and variation in binding energy of complex, probably correspond to conformational alteration of binding residues due to flap mutations.

Solvent accessibility of amino acids involved in structural and functional role for native and mutants of HIV-1 protease was analyzed. The occupancy of inhibitor during docking process further indicates the flexible behavior of residues of mutant structure. It proves that the increased flexibility govern by point mutation enable resistance behavior. It further provoked us to study the dynamics to understand the flexible behavior of HIV-1 protease enzyme. Since the docking process is quite related to binding residues so we have highlighted root mean square fluctuation of C-alpha carbon of binding residues in molecular dynamics simulation.

The RMSD of the backbone atoms of the protein from the starting structure over the course of simulation may be used as a measure

of the conformational stability of a protein during that simulation. The two phenomenons, variation in RMSD value of residues in 3D space and decrease level of binding energy is due to mutation at flap residual position 54th. We confirmed the above observation by studying the RMSF of binding residues. Compare to mutants, native structure shown less deviation with respect to time. Hence native have highest docking score and good interaction energy with Darunavir.

Root mean-square fluctuations (RMSF) analysis helps to understand the molecular flexibility nature of C-alpha carbon atom of binding residues which could influence the binding affinity toward the ligand molecule. A more detailed picture of differences in residue mobility within and between simulations can be obtained from graphs of the RMSF of Ca atoms relative to the average structure. Native has highest docking score and lowest fluctuation at alpha carbon atom of binding residues as compared to other two of mutants studied namely, mutant 1 and mutant 2. Mutant 2 showed the least docking score, thereby, expressing high fluctuation in the C-alpha carbon atom.

During whole simulation, native structure showed less fluctuation. This integral behavior of native HIV-1 protease gives good accommodation to inhibitor inside the pocket and better interaction with it. Hence native has significant susceptibility toward Darunavir. But flap mutations at 54th position to leucine/methionine are able to alter the structural position of binding residues from normal. Mutants have shown less interaction energy, docking score and more fluctuation of binding residues then native. Thus in-vitro, mutants have considerable amount of Darunavir resistance.

Conclusion

In this study, mechanism of Darunavir resistance flap mutants and dynamics of HIV-1 protease binding residues conformations was investigated using molecular dynamics simulations. Our analysis revealed docking score with Darunavir varied from 7556 to 6880. Decrease in docking score suggested the alteration of binding residues in 3D space. RMSD and RMS fluctuation values with respect to native type supported the docking score order. On the basis of docking calculation, binding energy and molecular dynamics simulation we conclude the resistance behavior of mutants was due to alteration in 3D structure at binding site residues.

The mutations at 54th position in flap region as a result of conformational change in binding residues often contribute to Darunavir resistance. However, several of these residues are not part of the active site cavity, and their essential role in causing drug resistance could possibly be rationalized if this conformational change actually occurs. Trapping HIV-1 protease in this inactive conformation would provide a unique opportunity for future drug design

The structures insight obtained with these simulations could be considered as a starting point for more refined all atom models and simulations aimed at designing drugs that target different sites far from the active one, suggesting novel therapeutic strategies.

References

1. Agarwal PK, Edelsbrunner H, Harer J, Wang Y (2004) Extreme elevation on a 2-manifold. Symp Comp Geo 20: 357-365.

2. Ahmad S, Gromiha M, Fawareh H, Sarai A (2004) ASAView: database and tool for solvent accessibility representation in proteins. BMC Bioinformatics 5: 51.

3. Berendsen HJC, Postma JPM, DiNola A, Hakk JR (1984) Molecular dynamics with coupling to an external bath. J Chem Phys 81:3684-3690.

4. Berendsen HJC, Postma JPM, Gunsteren WFV, Hermans J (1981) Interaction models for water in relation to protein hydration. B. Pullman (Ed.), Intermolecular Forces. D Reidel Publishing Company, Dordrecht 331-342.

5. Berman HM, Westbrook J, Feng Z, Gilliland G, Bhat TN, et al. (2000) The Protein Data Bank. Nucleic Acids Res 28: 235-242

6. Case DA, Pearlman DA, Caldwell JW, Wang J, Ross WS, et al. (2002) AMBER Simulation Software Package, version 7, Vol. 2006. San Francisco, CA: University of California.

7. Chothia C, Janin J (1975) Principles of protein-protein recognition. Nature 256: 705-708.

8. Clemente JC, Moose RE, Hemrajani R, Whitford LR, Govindasamy L, et al. (2004) Comparing the accumulation of active- and non-active-site mutations in the HIV-1 protease. Biochemistry 43: 12141–12151.

9. Coleman RG, Burr MA, Sourvaine DL, Cheng AC (2005) An intuitive approach to measuring protein surface curvature. Proteins 61: 1068-1074.

10. Coleman RG, Sharp KA (2006) Travel depth, a new shape descriptor for macromolecules: application to ligand binding. J Mol Biol 362: 441-458.

11. Collins JR, Burt SK, Erickson JW (1995) Flap opening in HIV-1 protease simulated by 'activated' molecular dynamics. Nat Struct Biol 2: 334-338.

12. Connolly ML (1983a) Analytical molecular surface calculation. J Appl Crystallogr 16: 548-558

13. Connolly ML (1983b) Solvent-accessible surfaces of proteins and nucleic acids. Science 221: 709-713.

14. Duhovny D, Inbar Y, Nussinov R, Wolfson HJ, (2005) PatchDock and SymmDock: servers for rigid and symmetric docking. Nucleic Acids Res 33: 363-367.

15. Duhovny D, Nussinov R, Wolfson HJ (2002) Lecture Notes in Computer Science. Springer-Verlag 2452: 185-200.

16. Dundas J, Ouyang Z, Tseng J, Binkowski A, Turpaz Y, et al. (2006) CASTp: computed atlas of   surface topography of proteins with structural and topographical mapping of functionally annotated resiudes. Nucleic Acids Res 34: 116-118.

17. Eckenhoff RG, Johansson JS (1997) Molecular interactions between inhaled anesthetics and proteins. Pharmacol Rev 49**:** 343-367.

18. Essmann U, Perera L, Berkowitz ML, Darden T, Lee H, et al. (1995) A smooth particle mesh ewald method. J Chem Phys 103: 8577-8593.

19. Feldman J, Snyder KA, Ticoll A, Pintilie G, Hogue CW (2006) A complete small molecule dataset from the protein data bank. FEBS Lett 580: 1649-1653.

20. Fraczkiewicz R, Braun W (1998) Exact and Efficient Analytical Calculation of the Accessible Surface Areas and Their Gradients for Macromolecules. J Comp Chem 19: 319-333.

21. Getzoff ED, Cabelli DE, Fisher CL, Parge HE, Viezzoli MS, et al., (1992) Faster Superoxide Dismutase Mutants Designed by Enhancing Electrostatic Guidance. Nature 358: 347-351.

22. Ghosh AK, Dawson ZL, Mitsuya H (2007) Darunavir, a conceptually new HIV-1 protease inhibitor for the treatment of drug-resistant HIV. Bioorg Med Chem 24:7576-7580.

23. Gilis D, Rooman M (1996) Stability changes upon mutation of solvent-accessible residues in proteins evaluated by database-derived potentials. J Mol Biol 257: 1112-1126.

24. Gilis D, Rooman M (1997) Predicting protein stability changes upon mutation using database-derived potentials: solvent accessibility determines the importance of local versus non-local interactions along the sequence. J Mol Biol 272: 276-290.

25. Gunsteren WFV, Billeter SR, Eising AA, Hunenberger PH, Kruger P, et al. (1996) Biomolecular Simulation: The Gromos 96 Manual and User Guide, Zurich, Switzerland: Hochschulverlag AG an der Zurich.

26. Han LY, Lin HH, Li ZR, Zheng CJ, Cao ZW, et al. (2006) PEARLS: program for energetic analysis of receptor-ligand system. J Chem Inf Model 46: 445-50.

27. Harrison RW, Weber IT (1994) Molecular dynamics simulation of HIV-1 protease with peptide substrate. Protein Eng 7: 1353-1363.

28. Hess B, Kutzner C, Spoel D, Lindahl E (2008) GROMACS 4: Algorithms for highly efficient, load-balanced, and scalable molecular simulation. J. Chem Theory Comput 4: 435-447.

29. Jacob NI (1992) Intermolecular and Surface Forces, Second Edition, Academic Press, New York.

30. Johnson V, Brun-Ve´zinet F, Clotet B, Günthard HF, Kuritzkes DR, et al. (2008) Update of the Drug Resistance Mutations in HIV-1: December 2008. Top HIV Med 16: 138-145.

31. Kervinen J, Thanki N, Zdanov A, Tino J, Barrish J, et al. (1996) Structural Analysis of the Native and Drug-Resistant HIV-1 Proteinases Complexed with an Aminodiol Inhibitor. Protein Pept Lett 3: 399.

32. King NM, Moses PJ, Nalivaika EA, Wigerinck P, Béthune M-P, et al. (2004) Structural and Thermodynamic Basis for the Binding of TMC114, a Next-Generation Human Immunodeficiency Virus Type 1 Protease Inhibitor. J Virol 78: 12012-12021.

33. Kohl NE, Emini EA, Schleif WA, Davis LJ, Heiman JC et al. (1988) Active human immunodeficiency virus protease is required for viral infectivity. Proc Natl Acad Sci USA 85: 4686–4690.

34. Liang J, Edelsbrunner H, Woodward C (1998) Anatomy of protein pockets and cavities: measurement of binding site geometry and implications for ligand design. Protein Sci 7:1884-1897.

35. Lindahl E, Azuara C, Koehl P, Delarue M (2006) NOMAD-Ref: visualization, deformation and refinement of macromo-lecular structures based on all-atom Normal ModeAnalysis. Nucleic Acids Res 34: W52-56.

36. Liu H, Muller-Plathe F, van Gusteren WF (1996) A combined quantum/classical molecular dynamics study of the catalytic mechanism of HIV protease. J Mol Biol 261:454–469.

37. Meagher KL, Carlson HA (2005) Solvation influences flap collapse in HIV-1 protease. Proteins 58: 119-125.

38. Miller M, Schneider J, Sathyanarayana BK, Toth MV, Marshall GR, et al. (1989) Structure of complex of synthetic HIV-1 protease with a substrate-based inhibitor at 2.3 A resolution. Science 246: 1149-1152.

39. Naray-Szabo G, Ferenczy GG (1995) Molecular Electrostatics. Chem Rev 95: 829.

40. Nayal M, Honig B (2006) On the nature of cavities on protein surfaces: application to the identification of drug bidning sites. Proteins 63: 892-906.

41. Politzer P, Muray JS (1991) Molecular electrostatic potentials and chemical reactivity. Reviews in Computational Chemistry 2: 273-312.

42. Rick SW, Erickson JW, Burt SK (1998) Reaction path and free energy calculations of the transition between alternate conformations of HIV-1 protease. Proteins 32: 7-16.

43. Sayle RA, Millner-White EJ (1995) Rasmol-biomolecular graphics for all. Trends Biochem Sci 20: 374-376.

44. Scott WRP, Schiffer CA (2000) Curling of flap tips in HIV-1 protease as a mechanism for substrate entry and tolerance of drug resistance. Structure 8: 1259-1265.

45. Shrake A, Rupley JA (1973) Environment and exposure to solvent of protein atoms. Lysozyme and insulin. J Mol Biol 79: 351-371.

46. Spoel D, Lindahl E, Hess B, Groenhof G, Mark AE, et al. (2005) GROMACS: fast, flexible, and free. J Comput Chem 26:1701-1718.

47. Thompson JD, Higgins DG, Gibson TJ (1994) CLUSTAL W: improving the sensitivity of progressive multiple sequence alignment through sequence weighting, position-specific gap enalties and weight matrix choice. Nucleic Acids Res 22: 4673-4680.

48. Trylska J, Grochowski P, McCammon JA (2004) The role of hydrogen bonding in the enzymatic reaction catalyzed by HIV-1 protease. Protein Sci 13: 513-528.

49. Wensing AM, van Maarseveen NM, Nijhuis M (2010) Fifteen years of HIV Protease Inhibitors: raising the barrier to resistance. Antiviral Res 85: 59-74

50. Wlodawer A, Miller M, Jaskolski M, Sathyanarayana BK, Baldwin E, et al. (1989) Conserved folding in retroviral proteases: crystal structure of a synthetic HIV-1 protease. Science 245: 616-621.

51. Zhang C, Vasmatzis G, Cornette JL, DeLisi C (1997) Determination of atomic desolvation energies from the structures of crystallized proteins. J Mol Biol 267: 707-726.